Seismic Behavior of High Strength Reinforced Concrete Columns Under Reversed Cyclic Loading

H. Bechtoula, Y. Mehani, A. Kibboua, M. Naili
National Earthquake Engineering Research Center, C.G.S, Rue Kaddour RAHIM, BP 252 Hussein Dey, Algiers, ALGERIA.

S. Kono, F. Watanabe
Kyoto University, Department of Architecture, Katsura campus, Dept. of Architecture, Nishikyo, Kyoto 615-8540, JAPAN

SUMMARY:
Experimental and analytical study on the seismic behavior of High Strength Reinforced Concrete columns under reversed cyclic loading is presented. In total six cantilever columns with the same shear span ratio and different sizes and concrete compressive strengths were tested at Kyoto University. Concrete compressive strength was 80, 130 and 180MPa. The tests demonstrated that, for specimens made of 180MPa, spalling of cover concrete was very brittle followed by a significant decrease in strength. Curvature was much important for the small size than for the medium size columns. Concrete compressive strength had an effect on the drift corresponding to the peak moment and on the equivalent viscous damping variation. Simple equation is proposed for evaluating the moment-drift envelope curves for the medium size columns knowing those of the small size columns. Experimental moment-drift and axial strain-drift histories were well predicted using a fiber model developed by the authors.

Keywords: Column, High strength concrete, Performance, Scale effect, Damping factor, Curvature, Damage

1. INTRODUCTION

With the increased knowledge that has been gained with respect to material availability, design methodology, and construction techniques, the feasible realm of high-strength concrete applications has grown dramatically. In the 1950s, concrete with a compressive strength of 34 MPa was considered high strength. Today, high strength concrete is defined as concrete with a specified compressive strength of 55 MPa or higher (ACI Committee-363 2005). In many markets today, concrete having a specified compressive strength in excess of 69 MPa is routinely produced on a daily basis. Although 55 MPa was selected as the current lower limit, it is not intended to imply that any drastic change in material properties or in production techniques occurs at this compressive strength. In reality, all changes that take place at or above 55 MPa represent a process which starts with the lower strength concretes and continues into the high strength realm. In Japan, use of Reinforced Concrete (RC) structures to high-rise buildings has rapidly increased after the publication of the report of "New RC Project" (JICE, 1988-1993). This project also took into account the results of many research program carried in the past (Nishiyama, 1993; Kuramoto, 1995 and Muguruma, 1990). The results of "New RC Project" and the succeeding progress of structural analyses and construction technology have made the realization of high-rise buildings of RC structures more possible.

Six high strength reinforced concrete columns with different sizes and concrete compressive strengths were tested under vertical and lateral loadings. This paper reports some of the main results drawn from this experiment

2. MATERIAL CHARACTERISTICS AND TEST SETUP

In total six high strength reinforced concrete cantilever columns, were designed according to the Japanese guide lines (AIJ, 1999) and tested at Kyoto University. Three specimens had a cross section of 325x325mm, named small size columns, and the three others had a cross section of 520x520mm,

named medium size columns. Fig. 2.1 shows the geometry and the dimensions of the medium size columns. The test variables were the column dimensions and the concrete compressive strength. Shear span ratio, longitudinal and transversal reinforcement and the normalized axial load were the same for the medium and small columns. Three types of concrete strength were used in the experiment, 80, 130 and 180MPa. Table 2.1 summarizes the specimen characteristics and the test variables. Concrete and steel mechanical characteristics are shown in Table 2.2.

Medium size columns where tested horizontally due to the high axial load, see Fig. 2.3. Two 8MN hydraulic jacks were used to apply the axial load and two 2MN jacks to apply the reversed cyclic loading. Small size columns were tested vertically using the steel testing frame to apply the axial load, see Fig. 2.2. The applied reversed cyclic loading history during the test for the 6 specimens is shown in Fig. 2.4.

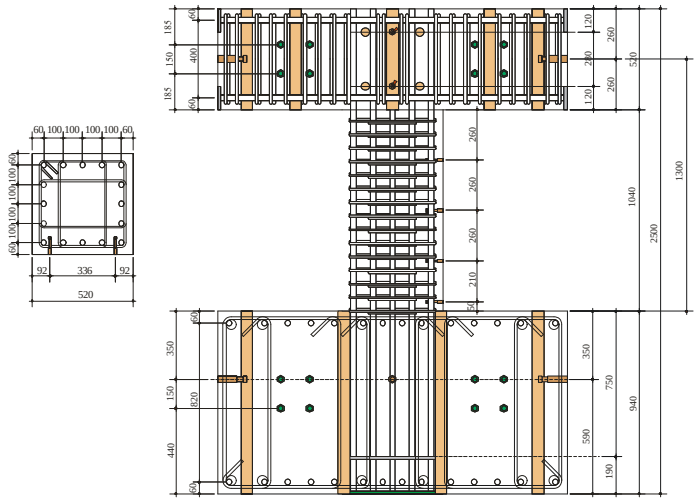

Figure 2.1: Dimensions and steel arrangement of the medium size specimens

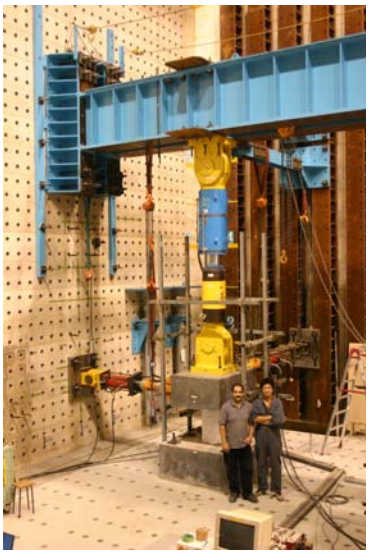

Figure 2.2: Test setup for the small size columns

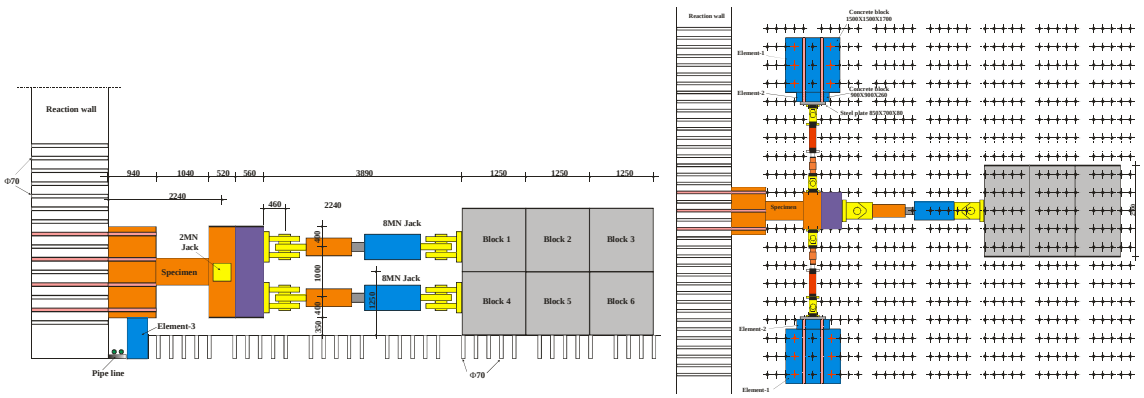

(a) Side view (b) Top view

Figure 2.3: Test setup for the medium size columns

Table 2.1: Specimens characteristics and test variables

Specimen	Column width D (mm)	Shear span (mm)	Shear span ratio	Concrete strength f'c (MPa)	Longitudinal rebar (ratio)	Shear rebar (ratio)	Normalized axial load ($N/f'cD^2$)
M180	520	1300	2.5	180	16D26 3.00 %	UD10@50 0.78 %	0.3
M130	520	1300		130			
M080	520	1300		80			
S180	325	812.5		180	16D16 3.00 %	UD6@50 0.78 %	
S130	325	812.5		130			
S080	325	812.5		80			

Table 2.2: Material characteristics

(a) Steel reinforcements

Identification	σy (Mpa)	σb (Mpa)	Es ($X10^5$) (Mpa)
SD 685 (D16)	757	967	1.95
SD 686 (D25)	729	925	1.96
UD6	964	1005	2.07
UD10	920	986	2.01

(b) Reinforced concrete

Specimen	Concrete strength (Mpa)	Ec (GPa)
M180	168	45.7
M130	131	43.1
M080	65.5	36.2
S180	170	46.5
S130	132	43
S080	68.2	34.8

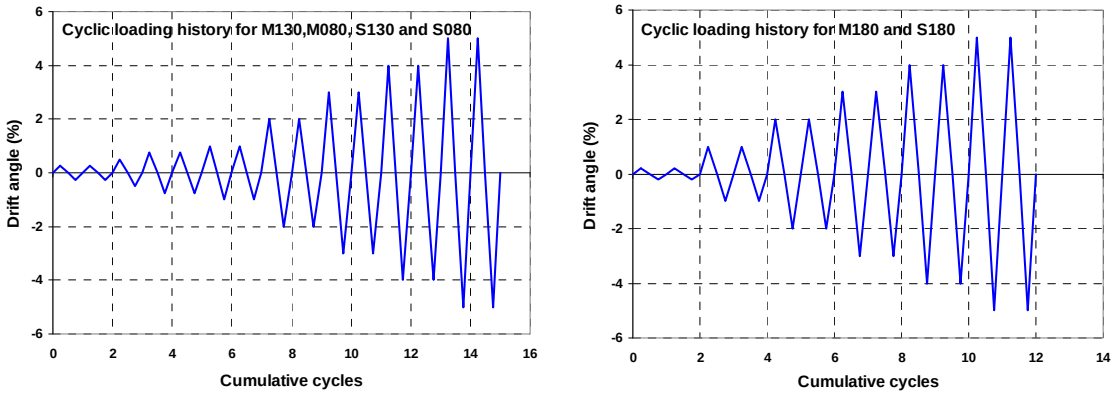

Figure 2.4: Loading history

3. EXPERIMENTAL RESULTS

3.1 Load-drift and axial strain variation

Experimental horizontal load-drift and axial strain-drift are illustrated in Fig. 3.1 and Fig. 3.2 for M080 and S080 column, respectively. Axial strains were measured using the displacement gauges set at the lower part of the columns shown in Fig. 3.5. Spalling of the concrete cover was very brittle especially for specimens with 130 and 180MPa. These stages are indicated with dot marks on the load-drift relationship curves. After the spalling, the horizontal bearing capacity of specimens with 130 and 180MPa concrete strength decreased significantly. However, for specimens M080 and S080 the horizontal load increased after spalling of the cover concrete.

The right side of Fig. 3.1 and Fig. 3.2 show the axial strain variation (shortening and/or elongation) measured at the center of the column. Shortening of the column has a positive sign in the figures. It was shown that when the concrete compressive strength of the specimen increases, only shortening is observed. In the same time it was observed that for a concrete compressive strength of 80MPa, small size column S080 showed both shortening and elongation, where medium size column M080 showed nearly only shortening.

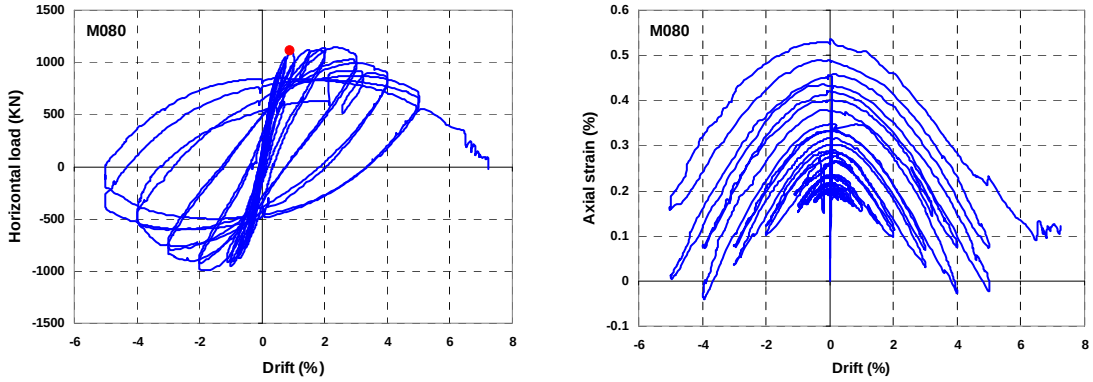

Figure 3.1: Load-drift and axial strain-drift relationships M080 column

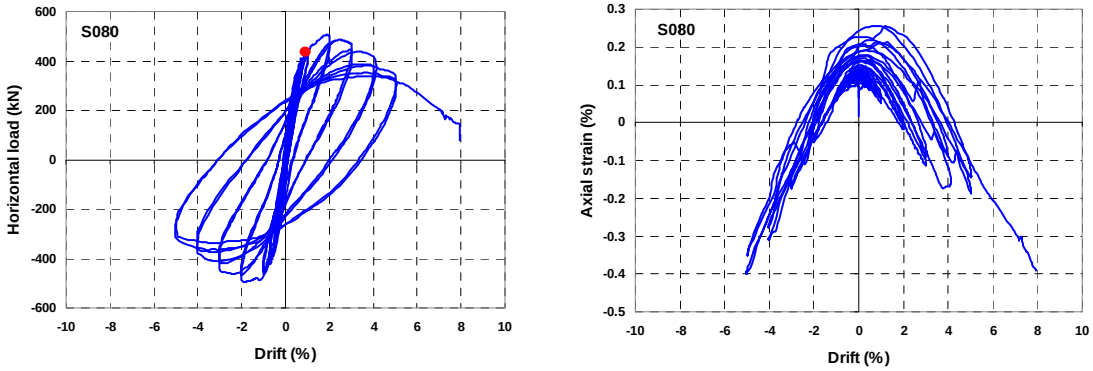

Figure 3.2: Load-drift and axial strain-drift relationships for S080 column

3.2 Size and concrete strength effects on the normalize moment-drift curves

Size effect on the moment-drift envelope curves was studied by comparing the normalized envelope curve of the medium size and the small size columns with the same concrete compressive strength. The normalization was done by dividing the original envelope curve by the maximum peak moment, $M_{\max}$.

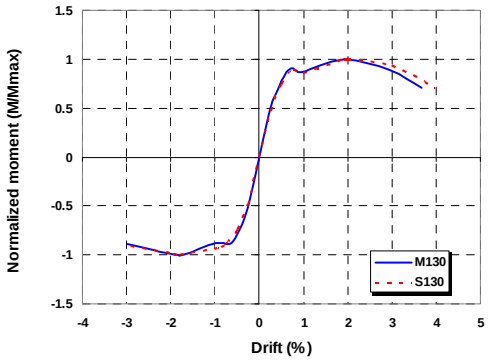

Figure 3.3: Size effect on the moment-drift relationships for M130 and S130

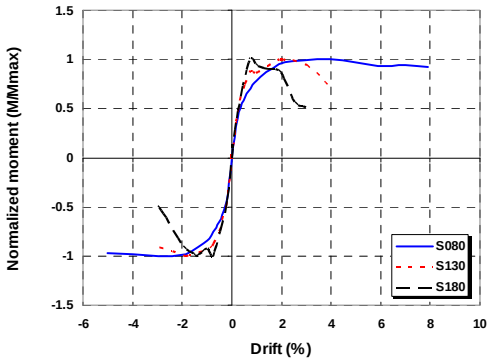

Figure 3.4: Concrete compressive strength effect on the moment-drift relationships

Fig. 3.3 shows a comparison between M130 and S130 columns in term of the normalized moment-drift envelope curves, where a slight difference can be seen. Effect of concrete compressive strength on the normalized moment-drift was clearly observed as illustrated in Fig. 3.4 for the small size columns, as an example. The authors observed that the drift corresponding to the maximum moment decreased with an increase in the concrete compressive strength. Also, slope of the descending branch increased with an increase in the concrete compressive strength.

3.3 Curvature-drift variation

In total 15 displacement gauges were set at the lower part of the column to measure the imposed deformations as shown in Fig. 3.5. Curvature was computed for a height equal to the column depth, D, for all specimens. It was observed that the measured curvature for the small size columns was higher than that measured for the medium size columns which can be seen from Fig. 3.6. This statement can be illustrated schematically as shown in Fig. 3.7.

However, for different values of concrete compressive strengths, and as shown in Fig. 3.8 for the medium size columns as an example, no differences were observed in term of curvature variation for a drift between -2% and +2%.

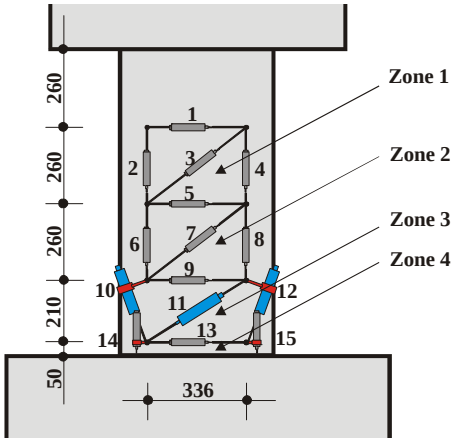

Figure 3.5: Displacement gauges locations

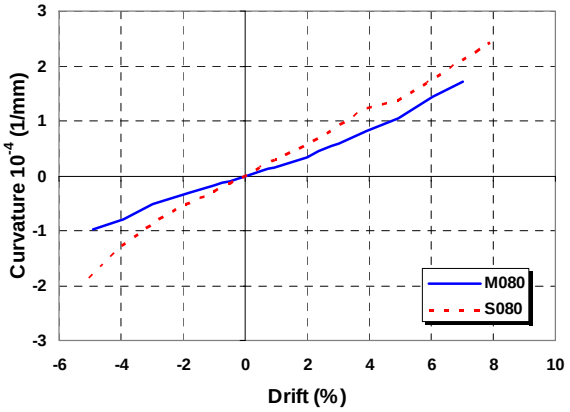

Figure 3.6: Curvature variation for M080 and S080

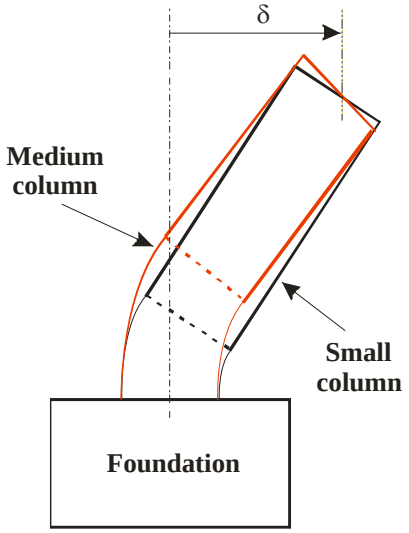

Figure 3.7: Illustration of the observed deformation between the medium and small size columns

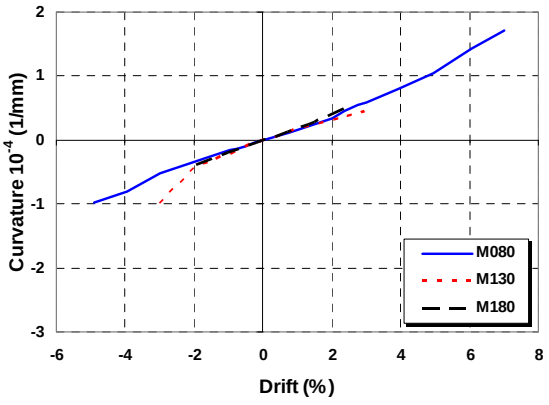

Figure 3.8: Concrete compressive strength effect on curvature-drift variation

3.4 DAMPING FACTOR VARIATION

Variation of the equivalent viscous damping factor was computed using the first cycle loops to each of the imposed drift angle (Shibata, 1976). The equivalent viscous damping, H_{eq}, was computed using the following expression:

$$H_{eq} = \frac{1}{4\pi}\frac{\Delta W}{W_e} \tag{4.1}$$

where: ΔW is the area enclosed by one cycle of hysteresis loop and W_e is the equivalent potential energy.

Variation of the equivalent viscous damping is shown in Fig. 3.9 for the small and the medium size column. From these two figures it can be drawn that the equivalent viscous damping increases with an increase in the concrete compressive strength. This increase can be attributed to the observed brittle failure of the reinforced concrete.

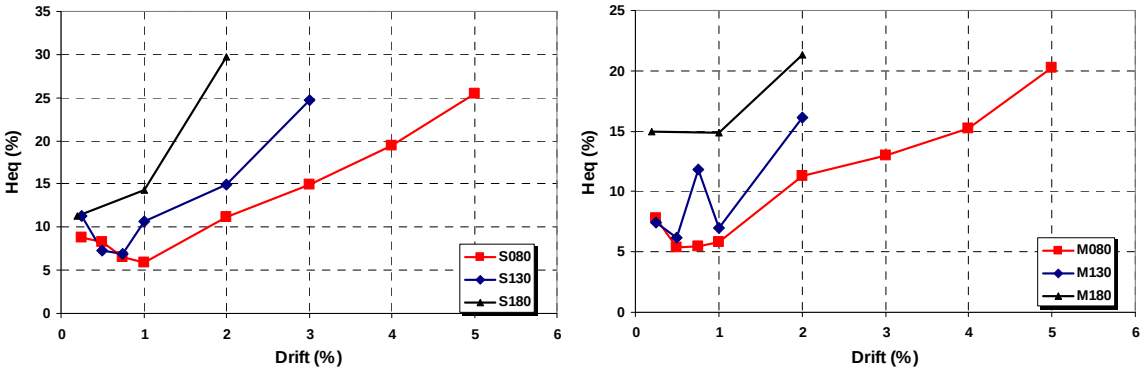

(a) Small size (b) Medium size

Figure 3.9: Effect of concrete compressive strength on the damping factor variation

3.5 Observed damage

In general, the small size columns suffered less damage than the medium size columns as shown in Fig. 3.10. This statement was also observed in the past by the first author (Bechtoula, 2005) while testing reinforced concrete columns with a concrete compressive strength varying between 30 and 40MPa.

Fig. 3.10 shows that for the small size columns, damage is concentrated at the lower part for a height less than the column depth, D. Whereas for the medium columns, the damage spreads for an average distance equal to 1.5D in height. This observation is accordance with the illustration shown previously in Fig. 3.7.

(a) M080

(b) S080

Figure 3.10: Columns states at the end of the test

3.6 Prediction of the moment-drift relationship

A relationship in terms of moment-drift envelope curves between the medium and the small size columns was established having the form of:

$$M_M / M_S = \left(D_M / D_S\right)^{\beta} \tag{3.1}$$

where M_M, M_S, D_M and D_S are the moment and the column depth for the medium and small size columns, respectively. β is a factor depending on the concrete compressive strength f_c', represented in Fig. 3.11, and given by Eqn. 3.2.

$$\beta = 0.0035\, f_c' + 3.13\,(in\ MPa) \tag{3.2}$$

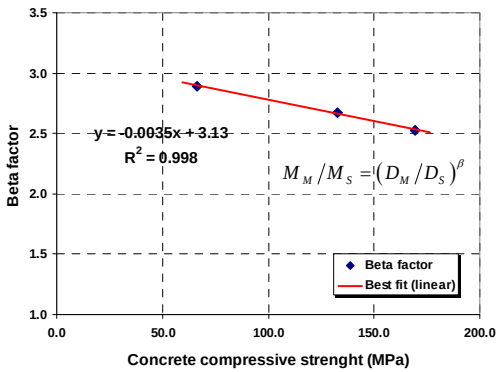

Figure 3.11: Determination of the "Beta" factor using the peak moment

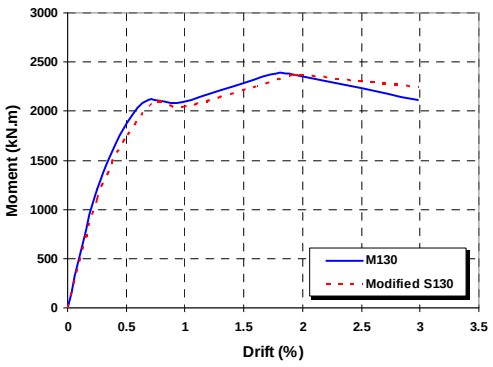

Figure 3.12: Prediction of the moment-drift envelope cure of the medium size columns

Eqn. 3.2 was evaluated using the peak moments in Eqn. 3.1 for the 3 types of reinforced concrete strengths. Fig. 3.12 shows a comparison between the moment-drift envelope curve of the medium size columns, M130, and the modified moment-drift envelope curves of the small size columns, S130, were using the above proposed equations. As it can be observed, a good agreement is obtained along the full loading history.

4. ANALYTICAL RESULTS

Behavior of a plastic hinge zone was predicted using a simple fiber model developed in our laboratory. Section analysis was carried out assuming Bernoulli's theory (plane sections remain plane) for concrete and longitudinal steel. The column cross section was subdivided into concrete fiber elements and reinforcing steel fiber elements. Section response was obtained by integrating all fiber element stresses and stiffness. Steel fiber elements followed Nakamura's stress-strain relation (Nakamura, 1977), whereas concrete fiber elements followed Popovic's stress-strain relation (Popovics, 1997). Concrete strength enhancement was taken into account using Sakino's et al. equation (Sakino, 1994). More details about this fiber model can be found elsewhere (Bechtoula, 2003).

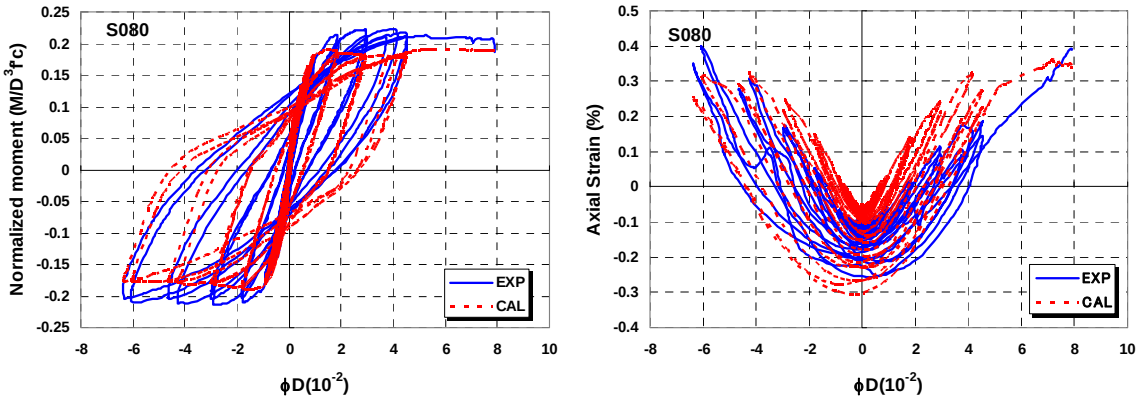

Figure 4.1: Fiber model and test results for S080 column

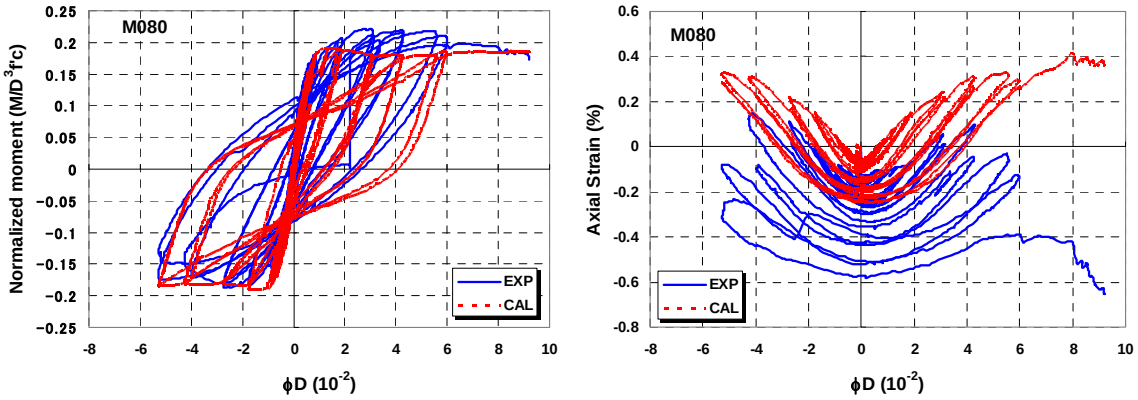

Figure 4.2: Fiber model and test results for M080 column

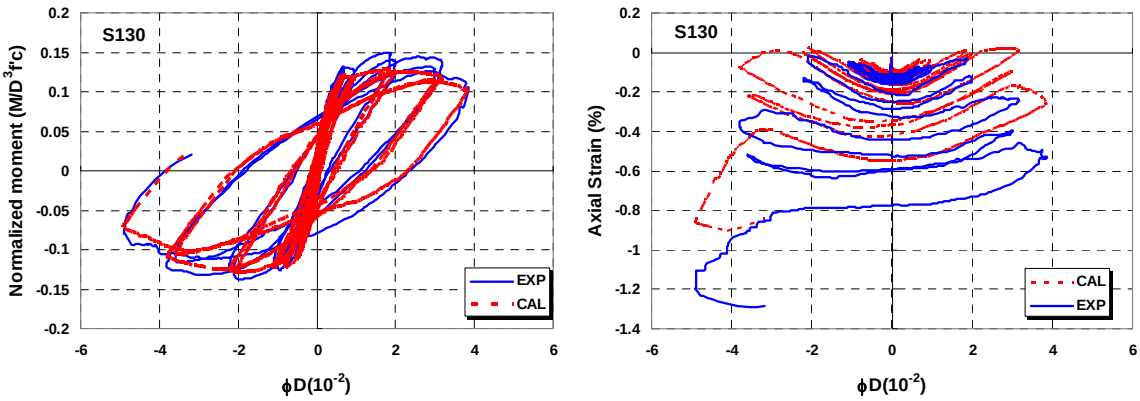

Figure 4.3: Fiber model and test results for S130 column

As an example, Fig. 4.1 through Fig. 4.3 show a comparison between the test and the fiber model results in term of moment-drift and axial strain-drift relationships for S080, M080 and S130 column, respectively.

As a general trend, a good estimation was obtained especially for the moment-drift relationships of the 6 specimens. However, analytical axial strain for the medium size columns (M080, M130 and M180) underestimated the experimental results, as illustrated on the right side of Fig. 4.2

5. CONCLUSIONS

To investigate the seismic performance of high strength reinforced concrete columns under cyclic loadings, six specimens of which three had a cross section of 325x325mm and the three other had a cross section of 520x520mm were designed, constructed and tested at Kyoto University. Design concrete compressive strength was 80, 130 and 180MPa. Shear span ratio and normalized axial load were identical for the six specimens. The experimental results showed that for specimens made of 180MPa concrete compressive strength, spalling of cover concrete was very brittle followed by a significant decrease in strength.

Curvature, evaluated at the base of the column for a height equal to the column depth, was much important for the small size columns than for the medium size columns. This difference in curvature distribution is attributed to the scale effect. Concrete compressive strength had no effect on the curvature distribution for a drift ratio varying between -2% and 2%, but it had an effect on the drift corresponding to the peak moments which decreased while the concrete compressive strengths increased. Also, an increase of the concrete compressive strength is followed by an increase of the equivalent viscous damping.

An equation was suggested for evaluating the moment-drift envelope curves for medium size columns using those obtained from small size columns. This equation was used for the three columns with different concrete compressive strengths and gave very good results. The main feature of this equation is its simplicity in practice, since it is based only on the geometrical and material characteristics of the columns.

Analytical investigation was carried out using a fiber model developed by the authors. Moment-drift and axial strain-drift hysteresis curves were predicted with a good accuracy using the fiber model. However, inaccurate analytical axial strain values were obtained for the medium size columns.

ACKNOWLEDGMENT

The authors are thankful to Mr. M. SAKASHITA, Mr. S. SHIBATA, Mr. T. MATSUDA, Mr. M. ODA and Mr. N. RYU former students at Kyoto University. The authors also acknowledge TAISEI and KAJIMA companies for their financial support. The first author is grateful to JSPS for their 2 years financial support as Post Doctor at Kyoto University.

REFERENCES

ACI Committee 363 (2005). High-Strength Concrete (ACI 363R) by ACI Committee 363 – High-Strength Concrete, *Seventh International Symposium on the Utilization of High-Strength/High-Performance Concrete*, Special publication SP-228-5, Washington, D.C., USA.

AIJ, 1999. Design guidelines for earthquake resistant reinforced concrete buildings based on inelastic concept. Architecture Institute of Japan, AIJ.

Bechtoula H. (2005). Seismic Performance of Moderate or Low Rise Reinforced Concrete Frame Buildings. *PhD thesis*, Department of Architecture and Architectural Engineering, Kyoto University, Japan.

Bechtoula H., Kono S., Sakashita M. and Watanabe F. (2003). Effect of number of cycles on damage progress

for large scale columns under multiaxial loadings. *Proceedings of Japan Concrete Institute, JCI, Kyoto*, **Vol. 25,** No.2, 355-360, Japan 16-18 July.

JICE (1988-1993). New RC Research Development Report 1988-1993. Japan Institute of Construction Engineering.

Kuramoto H., Kabeyasawa T., and Shen F. H. (1995). Influence of axial deformation on ductility of high-strength reinforced concrete columns under varying triaxial forces. *ACI structural journal*, **V.92**, No.5, 610-618.

Muguruma H. and Watanabe F. (1990). Ductility Improvement of High-Strength Concrete Columns with Lateral Confinement. *Proceeding of the Second International Symposium on Utilization of High-Strength Concrete*. University of California, Berkeley, May 20-23.

Nakamura T. and Yokoo Y. (1977). Non-stationary hysteresis uniaxial stress-strain relations of wide flange steel: Part II-Empirical formulas. *Transaction of the Architectural Institute of Japan, AIJ*. **N°.260**, 71-82, October.

Nishiyama, M. (1993). Axial loading test on high strength concrete prisms confined by ordinary and high strength steel. Utilization of high strength concrete. *Proceeding of High Strength Concrete Symposium*. Norway, 322-329.

Popovics S. (1997). A numerical approach to the complete stress-strain curve of concrete. *Journal of Cement and concrete research*. **Vol.3**, N°.5, 583-599, September.

Sakino K. and Sun Y. (1994). Stress-Strain curve of concrete confined by rectilinear hops. *Journal of structural and construction engineering.* Architectural Institute of Japan**, No. 461**, 95-104, Jul.

Shibata A., Sozen M. A. (1976). Substitute-Structure Method for Seismic Design in R/C. *Journal of the Structural Division, ASCE*. **Vol.102**, No.ST1, 1-18.